



HAL
open science

The role of climate and biotic factors in shaping current distributions and potential future shifts of European *Neocrepidodera* (Coleoptera, Chrysomelidae)

Francesco Cerasoli, Wilfried Thuiller, Maya Guéguen, Julien Renaud, Paola d'Alessandro, Maurizio Biondi

► To cite this version:

Francesco Cerasoli, Wilfried Thuiller, Maya Guéguen, Julien Renaud, Paola d'Alessandro, et al.. The role of climate and biotic factors in shaping current distributions and potential future shifts of European *Neocrepidodera* (Coleoptera, Chrysomelidae). *Insect conservation and diversity*, 2020, 13 (1), pp.47-62. 10.1111/icad.12376 . hal-02959776

HAL Id: hal-02959776

<https://cnrs.hal.science/hal-02959776>

Submitted on 7 Oct 2020

HAL is a multi-disciplinary open access archive for the deposit and dissemination of scientific research documents, whether they are published or not. The documents may come from teaching and research institutions in France or abroad, or from public or private research centers.

L'archive ouverte pluridisciplinaire **HAL**, est destinée au dépôt et à la diffusion de documents scientifiques de niveau recherche, publiés ou non, émanant des établissements d'enseignement et de recherche français ou étrangers, des laboratoires publics ou privés.



The role of climate and biotic factors in shaping current distributions and potential future shifts of European *Neocrepidodera* (Coleoptera, Chrysomelidae)

Journal:	<i>Insect Conservation and Diversity</i>
Manuscript ID	ICDIV-19-0099.R1
Manuscript Type:	Original Article
Date Submitted by the Author:	n/a
Complete List of Authors:	<p>Cerasoli, Francesco; Universita degli Studi dell'Aquila Dipartimento di Medicina Clinica Sanita Pubblica Scienze della Vita e dell'Ambiente, MeSVA - Environmental Sciences</p> <p>Thuiller, Wilfried; Universite Grenoble Alpes; Centre National de la Recherche Scientifique; Universite Savoie Mont-Blanc; Laboratoire d'Ecologie Alpine</p> <p>Gueguen, Maya; Universite Grenoble Alpes; Centre National de la Recherche Scientifique; Universite Savoie Mont-Blanc; Laboratoire d'Ecologie Alpine</p> <p>Renaud, Julien; Universite Grenoble Alpes; Centre National de la Recherche Scientifique; Universite Savoie Mont-Blanc; Laboratoire d'Ecologie Alpine</p> <p>D'Alessandro, Paola; Università degli Studi dell'Aquila Dipartimento di Medicina Clinica Sanità Pubblica Scienze della Vita e dell'Ambiente</p> <p>Biondi, Maurizio; Universita degli Studi dell'Aquila Dipartimento di Medicina Clinica Sanita Pubblica Scienze della Vita e dell'Ambiente, MeSVA - Environmental Sciences</p>
Keywords:	Habitat Suitability Models, Flea Beetles, <i>Neocrepidodera</i> , Climate Change, Ensemble Modelling, Host Plants

The role of climate and biotic factors in shaping current distributions and potential future shifts of European *Neocrepidodera* (Coleoptera, Chrysomelidae)

Running title: Drivers of *Neocrepidodera* distributions

Cerasoli, F.^{1*}, Thuiller, W.², Guéguen, M.², Renaud, J.², D'Alessandro, P.¹, Biondi, M.¹

¹ Department of Life, Health & Environmental Sciences, Univ. of L'Aquila, L'Aquila, Italy

² Univ. Grenoble Alpes, CNRS, Univ. Savoie MontBlanc, Laboratoire d'Ecologie Alpine (LECA), Grenoble, France

* Correspondence: Francesco Cerasoli, Department of Life, Health & Environmental Sciences, University of L'Aquila, Via Vetoio snc Coppito, 67100 L'Aquila, Italy

E-mail: francesco.cerasoli@univaq.it / francesco.cer91@gmail.com

ABSTRACT

- 1 1. The Western Palearctic species of *Neocrepidodera* Heikertinger (Coleoptera: Chrysomelidae:
2 Galerucinae: Alticini) mostly occur in medium and high elevation ecosystems particularly
3 sensitive to climate change.
- 4 2. Here, using ensemble projections from state-of-the-art habitat suitability modelling techniques,
5 we investigated how climate change and associated changes in host availability may affect the
6 persistence of three pairs of closely related *Neocrepidodera* taxa.
- 7 3. Modelled niches and suitability patterns reflected the current distributions of the targeted taxa.
8 *Neocrepidodera ligurica* occupies a small portion of the broader environmental niche of *N.*
9 *melanostoma*, and its narrow geographical range makes this species particularly vulnerable to
10 potential loss of suitable habitats in Western Alps. *Neocrepidodera cyanescens cyanescens* and
11 *N. cyanescens concolor* were found to occupy separate niches, but the non-significance of the
12 niche similarity test suggested their divergence being probably due to allopatric processes.
13 *Neocrepidodera corpulenta* and *N. rhaetica* showed partially overlapping niches, coherently
14 with their co-occurrence in Western Alps. Most of the targeted taxa were predicted to
15 potentially lose large portions of currently suitable areas in the forthcoming decades.

- 16 4. Notwithstanding the candidate host plants did not emerge as most important predictors, except
17 *Aconitum lycoctonum* for *N. cyanescens concolor*, a clear reduction of potential insect-plant co-
18 occurrence areas resulted for most future scenarios.
- 19 5. Climate was confirmed to noticeably affect the distribution of the targeted taxa, among which *N.*
20 *ligurica*, *N. cyanescens concolor*, *N. corpulenta* and *N. rhaetica* may need specific prioritization
21 measures in the future decades, claiming for further attention on mountainous entomofauna in a
22 warming world.

23
24 **Keywords:** Habitat Suitability Models, Flea Beetles, *Neocrepidodera*, Climate Change, Ensemble
25 Modelling, Host Plants

INTRODUCTION

26 The potential effects of ongoing and future human-related climate change on biodiversity at both
27 global and regional scales represent one of the most studied and debated issues of our epoch. More
28 and more evidence has been found that relates global warming to detrimental changes in both the
29 abiotic and biotic characteristics of a wide range of habitats, threatening a large number of animal
30 and plant species (Bellard *et al.*, 2012; Dullinger *et al.*, 2012; Zhang *et al.*, 2017; Archis *et al.*, 2018;
31 Iannella *et al.*, 2018). The species prevalently inhabiting mountainous regions severely suffer from
32 climate change, due to the associated rapid and dramatic modifications in the high-altitudes
33 ecosystems (Inouye, 2008; Forrest *et al.*, 2012; Li *et al.*, 2016; Urbani *et al.*, 2017; Rogora *et al.*,
34 2018). In this context, Habitat Suitability Models (HSMs) (Guisan *et al.*, 2017) represent a powerful
35 investigation tool, whose huge increase of implementations in the last two decades has marked a
36 noticeable break-through in conservation biogeography (Franklin, 2013). Indeed, the use of HSMs to
37 investigate the factors which shape the potential distribution of species showing puzzling
38 biogeographical patterns can provide useful insights (Acevedo *et al.*, 2012; Iannella *et al.*, 2017;
39 Reino *et al.*, 2017), especially in a climate change context.

40 The Alticini tribe comprises small-to-medium-sized phytophagous Coleoptera from the
41 Chrysomelidae family, subfamily Galerucinae, named ‘flea beetles’ because of the presence of a
42 metafemoral extensor tendon that enables them to jump. They are probably the largest and most
43 diversified tribe of Chrysomelidae, comprising about 550 genera and over 8000 species worldwide
44 (Nadein & Beždek 2014). Some genera spread over several zoogeographical regions, while others
45 are strictly endemic to narrow areas. Nonetheless, even when characterized by limited distributions,
46 genera or species-groups can differentiate in a high number of species (Biondi & D’Alessandro 2008,
47 D’Alessandro *et al.*, 2014, 2016). Host plants for the Alticini tribe are known from almost all the
48 vascular plant families, generally with high levels of specialization and close relation with the
49 vegetation types (Jolivet & Verma 2002; Biondi *et al.*, 2015; D’Alessandro *et al.*, 2018). The large
50 number of species, the diversification of distribution ranges, the differentiation capability, the close
51 relation with the vegetation types and the high levels of trophic specialization, make flea beetles
52 sensitive to various environmental changes. Thus, flea beetles represent a good model for the
53 investigation of evolutionary and biogeographical hypotheses and processes at different geographic
54 scales (D’Alessandro *et al.*, 2014, 2018; Urbani *et al.*, 2015, 2017).

55 The flea beetle genus *Neocrepidodera* Heikertinger (Coleoptera: Chrysomelidae: Galerucinae:
56 Alticini) is widespread, with about 100 species in the Palaearctic, Nearctic and Oriental regions. The
57 Palaearctic taxa were revised by Biondi (1989, 1993), Konstantinov (1991), Konstantinov and
58 Vandenberg (1996), Baselga and Novoa (2005), Baselga (2006) and Döberl (2010). This genus occurs
59 in Europe with 30 species, according to the Pan-European Species Directories Infrastructure (PESI,
60 2018). The Western Palaearctic species are generally associated with medium and high elevations,
61 and they show a high rate of endemism and vicariance deemed to be mainly linked with the
62 Quaternary paleoclimatic events (Biondi 1989, 1993).

63 Notwithstanding the noticeable peculiarities characterising the biogeography and ecology of these
64 phytophagous beetles, no previous study implementing HSMs has been carried out on any
65 *Neocrepidodera* species to investigate the relative distributional drivers.

66 Here, we used Ensemble Forecasting techniques (Araujo & New, 2007), which permit the
67 combination of multiple HSMs into a single Ensemble Model through different averaging criteria, to
68 assess the potential future responses of three pairs of *Neocrepidodera* taxa to different climate change
69 scenarios. Specifically, three Representative Concentration Pathways (RCPs), depicting increasing
70 radiative forcing due to human-induced greenhouse gas (GHG) emissions, were considered for model
71 projections.

72 Recent studies have highlighted the usefulness of including within the HSMs some predictors
73 representing biotic interactions (Hof *et al.*, 2012; Gherghel *et al.*, 2018; Paiva-Silva *et al.*, 2018)
74 and/or the response of the resources used by animal species to the same abiotic variables used to
75 model the species' potential distribution (Thuiller *et al.*, 2018). Thus, for two selected pairs of closely
76 related *Neocrepidodera* taxa, we implemented a nested modelling framework in which the predictions
77 from Ensemble Models (EMs) built for the candidate host plants were included as predictors in the
78 EMs built for the hosted flea beetles.

79 Moreover, we investigated, through measurements of niche overlap and statistical testing of niche
80 divergence (Warren *et al.*, 2008; Broennimann *et al.*, 2012), whether the current distribution patterns
81 characterizing the three pairs of *Neocrepidodera* taxa analysed could be linked to actual differences
82 in their environmental and/or resource requirements. Results from such niche analysis could be
83 helpful to clarify both the factors shaping the biogeography of the selected *Neocrepidodera* taxa and
84 the potential differences in their response to climate change resulting from the performed Ensemble
85 Forecasts.

MATERIALS AND METHODS

Study area and target taxa

87 The study area encompasses three major mountainous massifs, which host almost all the occurrence
88 records of the targeted taxa (Fig. 1): the Apennines, which run north-south across most of peninsular
89 Italy; the Alps, whose arc covers Southern France, Northern Italy, Switzerland, Austria, Southern
90 Germany and extends southeast in the Balkans; the Carpathians, going through Poland, Slovakia,
91 Czech Republic, Austria, Hungary, Ukraine, Romania and Serbia.

92 We focused the analyses on three pairs of *Neocrepidodera* species and subspecies:

- 93 1) *N. ligurica* J. Daniel, 1904 versus *N. melanostoma* Redtenbacher, 1849, with the latter occurring
94 in the Central and Northern Apennines, throughout the Alpine arc and in some localities of the
95 Dinaric Alps, and the former occupying a narrow portion of the *N. melanostoma* distribution in
96 the Ligurian, Maritime and Cottian Alps;
- 97 2) *N. cyanescens cyanescens* Duftschmid, 1825 versus *N. cyanescens concolor* K. Daniel, 1900, the
98 first spread across the Eastern Alps and present in some localities in the Carpathians and in
99 Transylvania, and the latter distributed in the Ligurian and Maritime Alps;
- 100 3) *N. corpulenta* Kutschera, 1860 versus *N. rhaetica* Kutschera, 1860; the former species is spread
101 all along the Apennines chain, and present in some localities in the Balkans, in the Carpathians,
102 in Transylvania and in the Western Alps, where it shares a parapatric zone with *N. rhaetica*, which
103 replaces *N. corpulenta* in the rest of the Alpine arc.

104 We analysed the above-mentioned *Neocrepidodera* taxa by pairs to assess if differential responses to
105 climatic and/or biotic factors could be linked to niche divergence phenomena between the closely
106 related taxa forming each pair. This way, the environmental drivers contributing to their current
107 disjunct (the two *N. cyanescens* subspecies), parapatric (*N. corpulenta* - *N. rhaetica*) or nested (*N.*

108 *ligurica* – *N. melanostoma*) distributions, as well as the potential shifts in response to climate change,
109 could be better characterized.

110 Occurrence records (GPS resolution or exact locality) for the target taxa were retrieved from Maurizio
111 Biondi's and other entomological collections, from the checklist of the Italian fauna (Biondi, 2006),
112 from literature search and from the GBIF (Global Biodiversity Information Facility) database. In the
113 latter case, occurrence records were scrutinized through both expert-based evaluation and literature
114 search about the localities reported to host *Neocrepidodera*, to check their coherence with the known
115 autoecology and biogeographical history of the considered taxa.

116 Considering available evidence about preferred host plants of some *Neocrepidodera* species (Biondi,
117 1993), we selected two species of Ranunculaceae, namely *Aconitum lycoctonum* L., 1753 emend.
118 Koelle and *A. napellus* L., 1753 emend. Skalický, as candidate host plants for *N. cyanescens*
119 *cyanescens* and *N. cyanescens concolor*, while for *N. corpulenta* and *N. rhaetica* we chose as
120 candidate hosts two species of Asteraceae, namely *Arnica montana* L., 1753 and *Doronicum*
121 *austriacum* Jacq., 1774. No plants were included as biotic predictors within the HSMs built for *N.*
122 *ligurica* and *N. melanostoma* because less evidence about preferred hosts of these species is available
123 so far.

124 Occurrence data for the selected plant species were gathered from the database of the CBNA
125 (Conservatoire Botanique National Alpin), containing georeferenced records (ETRS89 reference
126 system) from both France and other European countries; we considered only records with a minimum
127 resolution of 1 km temporally ranging from the middle 1960s to 2013. Since the presence points of
128 the *Neocrepidodera* taxa were recorded using the WGS84 geographic coordinate system, we
129 projected them to the ETRS89 reference system in ArcMap 10.0 (ESRI 2011) before model building;
130 thus, the occurrence datasets of *Neocrepidodera* and those of the candidate host plants shared the
131 same reference system. Fig. 1 shows the distribution of presence points retrieved for the

132 *Neocrepidodera* taxa and for the host plants, while coordinates and sources of these occurrence
133 records are listed in Supporting Information Table S1.

134 The available occurrences for each *Neocrepidodera* and plant taxon were spatially thinned through
135 the “spThin” R package (Aiello-Lammens *et al.*, 2015). For each taxon, three thinning iterations were
136 performed setting ‘thin.par’ = 2 km to rarefy occurrences falling within neighbouring cells of the
137 raster maps representing the considered predictors (see ‘Environmental variables’). Then, the thinned
138 dataframe with the highest number of remaining occurrences was selected for model building to
139 preserve as information as possible about environmental conditions at occurrence locations (Anderson
140 & Raza, 2010), given the limited amount of data available for some *Neocrepidodera* taxa (e.g. *N.*
141 *cyanescens concolor* and *N. ligurica*).

142 The full occurrence datasets were instead used to obtain a representation of the geographic range of
143 each *Neocrepidodera* taxon through α -hull-based polygons, drawn by means of the R package
144 “alphahull” (Beatriz Pateiro-López & Alberto Rodríguez-Casal, 2010), which are less affected by
145 biases in range estimates than the classic minimum convex polygons (Burgman & Cox, 2003).

146

Environmental variables

Current

147 Nineteen downscaled bioclimatic variables from Worldclim version 1.4 (Hijmans *et al.*, 2005;
148 Dullinger *et al.*, 2012) were chosen as climate-related candidate predictors and downloaded as raster
149 files at 30 seconds resolution (i.e. approximately 1 km²). The downloaded rasters were projected from
150 the original WGS84 reference system to ETRS89-LAEA (Lambert Azimuthal Equal Area) by means
151 of the ‘projectRaster’ function from the “raster” R package (Hijmans *et al.*, 2015), to match the metric
152 reference system of the occurrence data (ETRS89) and preserve cell extent across the full latitudinal
153 range of the study area.

154 Presence of multicollinearity within the set of candidate predictors, which may lead to distortions in
155 the estimation of model parameters and variable importance (Dormann, 2007; Crase *et al.*, 2012;
156 Dormann *et al.*, 2013), was first checked by calculating the Pearson r coefficient for each pair of
157 variables across the study area. For the pairs with Pearson $|r| > 0.7$, we kept the variable presumed
158 to be more relevant to the species' ecology (Dormann *et al.*, 2013; Brandt *et al.*, 2017). Since hidden
159 multicollinearity issues could still affect the data after having discarded the variables showing high
160 pairwise correlations across the study area, further refinement on the candidate predictors was
161 accomplished performing Variance Inflation Factor (VIF) analyses (Guisan *et al.*, 2006, 2017) on the
162 set of presence-pseudoabsence points used to build the HSMs (see 'Model building').

Future

163 Two time horizons (2050 and 2070) and three Representative Concentration Pathways (RCPs;
164 RCP2.6, RCP4.5 and RCP8.5) (Meinshausen *et al.*, 2011), based on the Rossby Centre Regional
165 Climate Model RCA4 (Strandberg *et al.*, 2014), were considered to investigate potential future
166 distributional shifts of the target *Neocrepidodera* taxa in response to increasing GHGs concentration
167 trajectories. As for the layers representing current climate, the WGS84-based rasters for the future
168 scenarios were projected to ETRS89-LAEA through the 'projectRaster' function.

Model building

169 Model building was performed in R (R Core Team, 2018) through the package "biomod2" (Thuiller
170 *et al.*, 2016). The algorithms selected to build the HSMs were Generalized Linear Model (GLM),
171 Generalized Additive Model (GAM) and Generalized Boosted Regression Models (GBM). For each
172 algorithm, two-way interactions among predictors were allowed. With respect to the other relevant
173 parameterization arguments, the default 'BIOMOD_ModelingOptions' settings were maintained for
174 GLM ('quadratic' formula type, binomial error distribution with logit link function, and stepwise AIC
175 as model selection criterium) and for GAM ('s_smoother' cubic-spline smoother and binomial error
176 distribution with logit link function). For GBM, we set 5-fold cross-validation with 5000 fitted trees

177 for each iteration, while other relevant parameters were maintained to the default values ('shrinkage'
178 = 0.001, 'bag.fraction' = 0.5).

179 For both the target *Neocrepidodera* taxa and the selected host plants, pseudoabsences (hereafter, PAs)
180 were generated by means of a geographical exclusion strategy. First, a buffer ranging from 2 km to
181 200 km around the thinned occurrences was generated for each taxon through the 'gBuffer' and
182 gDifference' functions of the "rgdal" R package (Bivand *et al.*, 2014). Then, 10000 PAs were drawn
183 at random within the obtained buffer polygon, after having clipped this latter to the boundaries of the
184 study area to avoid the generation of PAs within raster cells with no values for the predictors (i.e. at
185 sea). The clipping was performed through the 'Extract by Mask' function in ArcMap 10.0. Finally,
186 10 sets of 1000 PAs each were generated for HSMs calibration, randomly sampling without
187 replacement from the previously drawn 10000 PAs.

188 The choice of a geographically-buffered PAs sampling, as well as the number of PAs sets and the
189 sample size of these latter, was based on Barbet-Massin *et al.* (2012), who demonstrated that this
190 approach is well suited to the algorithms we selected and that it ameliorates HSMs' accuracy when
191 few occurrence records are available.

192 The chosen buffer distances were intended to avoid both the selection of PAs within the same cell of
193 a presence point, or from the immediately contiguous cells, and the selection of PAs too far from
194 presence localities. Indeed, PAs selected in a restricted region around occurrence localities would
195 have increased the probability of obtaining low performing HSMs (VanDerWal *et al.*, 2009); on the
196 other hand, the generation of PAs within a noticeably broad area would have increased the probability
197 of PAs falling in regions with bioclimatic conditions pronouncedly different than those of presence
198 localities, potentially leading to over-simplified and artificially accurate HSMs (Chefaoui & Lobo,
199 2008; VanDerWal *et al.*, 2009).

200 The PAs sets generated for each taxon and the respective thinned occurrences were then joined in a
201 single dataset and converted to biomod2-suited format by means of the 'BIOMOD_FormatingData'

202 function ('PA.strategy' set to 'user.defined'). Particularly, for each *Neocrepidodera* taxon and each
203 host plant, the dataset for HSMs building comprised 90% of the available thinned occurrences and
204 the ten sets of 1000 PAs previously generated. The remaining thinned occurrences were instead joined
205 with 100 additional PAs randomly drawn within the buffer polygon, excluding the 10000 PAs already
206 generated for model building, to build an independent evaluation dataset with which the continuous
207 habitat suitability (hereafter, HS) predictions from the Ensemble Model (hereafter, EM) could be later
208 compared to select a binarization threshold.

209 Values of the bioclimatic variables retained after the preliminary check of pairwise correlations, as
210 well as suitability values from the wmean EMs (see 'Model evaluation and Ensemble Forecast')
211 obtained for the candidate host plants, were extracted at occurrences and PAs points through the
212 'extract' function of the "raster" R package. Then, a VIF analysis was performed on these predictors
213 through the 'vif.step' function of the "usdm" R package (Naimi, 2015), and the ones exceeding the
214 recommended threshold of $VIF = 10$ (Guisan *et al.*, 2017) were discarded from the modelling
215 framework.

Model evaluation and Ensemble Forecast

216 Three iterations of a random split-sample cross-validation approach (Thuiller *et al.*, 2016; Guisan *et*
217 *al.*, 2017) were performed on the datasets generated for HSMs building, each time using 80% of the
218 data for model calibration and the remaining 20% as test data. Thus, 90 HSMs (i.e. 3 algorithms * 3
219 split-sample runs * 10 PAs sets) were finally built for each target taxon. Then, the HSMs whose
220 predictions on the test data reached a chosen threshold value for both the True Skill Statistic (TSS)
221 (Allouche *et al.*, 2006) and the Area Under the Curve (AUC) of the Receiver Operating Characteristic
222 Curve (ROC) (Fielding & Bell, 1997; Phillips *et al.*, 2006) were retained for the EM building process:
223 the selected thresholds were $TSS \geq 0.7$ and $AUC \geq 0.8$. In the ensemble modelling step, we used the
224 'weighted mean of probabilities' (wmean) and the 'coefficient of variation of probabilities' (cv)
225 algorithms implemented in the 'BIOMOD_EnsembleModeling' function. The wmean algorithm

226 represents a form of weighted averaging in which the more an HSM attains high discrimination scores
227 on test data the higher its predictions are weighted in the EM (Marmion *et al.*, 2009); here, the
228 contribution of the single HSMs to the wmean EM was weighted based on their TSS scores. The cv
229 EM, instead, provides information about the degree of uncertainty in the EM building process. Indeed,
230 it returns the coefficient of variation of HS values over the component HSMs (Thuiller *et al.*, 2016),
231 so that the higher the cv value at a certain pixel, the higher the variability in the HS values predicted
232 for that pixel by the different HSMs.

233 The algorithm-independent randomization procedure of the BIOMOD modelling framework
234 (Thuiller *et al.*, 2009) was used to calculate the contribution of the single predictors within the
235 obtained wmean EMs, setting the number of permutations to 3. Contribution scores from the 3
236 permutation runs were first averaged and then scaled to percent contributions (Bucklin *et al.*, 2015).

237 The wmean EM for each of the 6 future scenarios (2 time horizons * 3 RCPs) was computed by means
238 of the 'BIOMOD_EnsembleForecasting' function, projecting to that scenario the HSMs selected for
239 ensemble modelling and then weighting their predictions based on the weights they achieved in the
240 wmean EM built under current conditions. Successively, we used the 'BIOMOD_RangeSize'
241 function to investigate potential shifts in suitable areas for the target *Neocrepidodera* taxa and the
242 corresponding candidate host plants with respect to the current conditions (i.e. suitable areas lost,
243 remaining stable or gained). Since this function needs binarized predictions (i.e. suitable vs unsuitable
244 areas), we chose as binarization approach the maximisation of the TSS (max-TSS), computed by
245 means of the 'Find.Optim.Stat' function comparing the wmean EM continuous predictions with the
246 previously set-aside evaluation data. This is reported to be an appropriate binarization criterium when
247 dealing with presence-background HSMs (Liu *et al.*, 2013). The obtained thresholds are listed in
248 Supporting Information Text S1.

249 The binarized raster maps for the current scenario and those representing the predicted HS shifts
250 within the future scenarios were converted to shapefiles in ArcMap 10.0. Then, the 'Intersect'

251 function of ArcMap 10.0 was used to extract, for each *Neocrepidodera* - host plant pair, the overlap
252 polygons representing: 1) areas predicted to be suitable for both the considered flea beetle and the
253 corresponding host plant under the current scenario, and 2) the different combinations of the Stable
254 and Gain categories, representing areas predicted to be suitable in the projection scenario for both the
255 flea beetle and the candidate host. The extent of these overlap polygons was then computed to
256 quantify the effect of future warming conditions on the potential co-occurrence of the target
257 *Neocrepidodera* taxa and the respective candidate hosts.

Niche analysis

258 In order to understand how the relative positions of the considered *Neocrepidodera* taxa in the
259 environmental space could relate to their current distribution patterns, we implemented the ‘PCA-
260 env’ approach described in Broennimann *et al.* (2012). The set of input predictors used to build the
261 HSMs was thus reduced to two uncorrelated principal components, based on which kernel-smoothed
262 densities of occupancy of the taxa in the environmental space were built. Moreover, for each pair of
263 *Neocrepidodera* taxa, biplots were produced through the “factoextra” R package (Kassambara &
264 Mundt, 2017) to show the contribution of the input predictors along the two principal component
265 axes.

266 The Schoener’s *D* metric (Schoener, 1970; Warren *et al.*, 2008) was calculated, through the
267 ‘ecospat.niche.overlap’ function of the “ecospat” R package (Di Cola *et al.*, 2017), to assess the
268 degree of niche overlap within each pair of *Neocrepidodera* taxa. The obtained niche overlap values
269 were statistically tested first for the niche equivalency hypothesis (Warren *et al.*, 2008; Broennimann
270 *et al.*, 2012) through the ‘ecospat.niche.equivalency.test’ function, and then for the more conservative
271 niche similarity hypothesis (Warren *et al.*, 2008; Broennimann *et al.*, 2012) by means of the
272 ‘ecospat.niche.similarity.test’ function. For both tests, the observed niche overlap is compared to the
273 95th percentile of the null distribution built through the specific randomization procedure (1000

274 pseudo-replicates for both tests): if the observed D falls outside this interval, the null hypothesis can
275 be rejected.

276

RESULTS

277 Nine bioclimatic variables were retained as candidate predictors after the check for multicollinearity
278 across the entire study area (see Supporting Information Table S2): BIO2 (Mean diurnal temperature
279 range), BIO3 (Isothermality), BIO4 (Temperature seasonality), BIO5 (Maximum temperature of
280 warmest month), BIO6 (Minimum temperature of coldest month), BIO8 (Mean temperature of
281 wettest quarter), BIO17 (Precipitation of driest quarter), BIO18 (Precipitation of warmest quarter)
282 and BIO19 (Precipitation of coldest quarter). The VIF analyses successively performed on the
283 presence-pseudoabsence datasets led to the final sets of uncorrelated predictors listed in Table 1.

284 The number of residual occurrences after the spatial thinning for the target *Neocrepidodera* taxa and
285 the candidate hosts, along with the countries hosting these presence records, are reported in
286 Supporting Information Table S3, while Table 2 summarizes the percent importance scores obtained
287 for the relevant predictors within the Ensemble Models (EMs) built for the host plants and the
288 *Neocrepidodera*.

289

290 **Table 1.** Predictors selected to build the HSMs for the target *Neocrepidodera* taxa and the candidate host plants. HS = Habitat Suitability

Host plants	Predictors
<i>Aconitum lycoctonum</i> <i>Aconitum napellus</i> <i>Arnica montana</i> <i>Doronicum austriacum</i>	BIO3; BIO4; BIO6; BIO8; BIO18; BIO19
<i>Neocrepidodera</i>	Predictors
<i>N. ligurica</i> <i>N. melanostoma</i>	BIO3; BIO4; BIO6; BIO8; BIO18; BIO19
<i>N. cyanescens concolor</i> <i>N. cyanescens cyanescens</i>	BIO3; BIO4; BIO6; BIO8; BIO18; <i>Aconitum lycoctonum</i> HS; <i>Aconitum napellus</i> HS
<i>N. corpulenta</i> <i>N. rhaetica</i>	BIO3; BIO4; BIO6; BIO8; BIO18; BIO19; <i>Arnica montana</i> HS; <i>Doronicum austriacum</i> HS

291

292

293

Table 2. Averaged percent importance scores of: the three most contributing bioclimatic predictors for *Aconitum lycoctonum*, *Aconitum napellus*, *Arnica montana* and *Doronicum austriacum*; the four most contributing bioclimatic predictors for each target *Neocrepidodera* taxon, along with host plant Habitat Suitability (HS) for *N. cyanescens concolor*, *N. cyanescens cyanescens*, *N. corpulenta* and *N. rhaetica*.

294

Candidate Host Plants Ensemble Models					
Taxon	Predictor	Percent Contribution	Taxon	Predictor	Percent Contribution
<i>Aconitum lycoctonum</i>	BIO6	33.6	<i>Aconitum napellus</i>	BIO6	46.0
	BIO18	27.0		BIO8	37.1
	BIO8	18.5		BIO4	11.6
<i>Arnica montana</i>	BIO6	37.5	<i>Doronicum austriacum</i>	BIO6	39.0
	BIO4	21.6		BIO8	19.1
	BIO8	18.4		BIO4	16.0
Neocrepidodera Ensemble Models					
Taxon	Predictor	Percent Contribution	Taxon	Predictor	Percent Contribution
<i>N. ligurica</i>	BIO4	22.6	<i>N. melanostoma</i>	BIO6	34.4
	BIO6	21.0		BIO18	21.2
	BIO3	18.6		BIO4	18.7
	BIO19	16.5		BIO3	10.6
<i>N. cyanescens concolor</i>	<i>Aconitum lycoctonum</i> HS	28.7	<i>N. cyanescens cyanescens</i>	BIO18	43.3
	BIO6	18.9		BIO6	21.9
	BIO3	16.2		BIO2	9.3
	BIO18	14.0		BIO8	8.5
	BIO8	9.1		<i>Aconitum napellus</i> HS	8.1
	<i>Aconitum napellus</i> HS	4.5		<i>Aconitum lycoctonum</i> HS	2.1
<i>N. corpulenta</i>	BIO8	18.9	<i>N. rhaetica</i>	BIO6	19.9
	BIO3	18.0		BIO8	19.5
	BIO4	15.5		BIO3	14.2
	BIO19	13.8		BIO4	10.5
	<i>Arnica montana</i> HS	8.4		<i>Arnica montana</i> HS	9.0
	<i>Doronicum austriacum</i> HS	3.4		<i>Doronicum austriacum</i> HS	8.9

295 Apart from *Aconitum lycoctonum*, for which precipitation of the warmest quarter (BIO18) obtained
296 the second highest importance score, temperature-linked variables, particularly minimum
297 temperature of the coldest month (BIO6), clearly resulted as the most important predictors for all the
298 candidate host plants (Table 2). From the corresponding partial response curves, Habitat Suitability
299 (HS) for the host plants appears to decrease, once the remaining predictors have been set to their mean
300 value, as temperature, or its seasonality (BIO4), increases (Supporting Information Fig. S1).
301 Temperature-linked variables resulted as predominant predictors also for *N. ligurica* and *N.*
302 *melanostoma*, with the first species showing comparable importance scores for BIO4 and BIO6
303 (Table 2), and the latter being instead more markedly dependent upon BIO6. Different partial
304 responses to BIO6 emerged for the two species, with the response curve obtained for *N. ligurica* being
305 monotonically decreasing and the one obtained for *N. melanostoma* being more bell-shaped-like
306 (Supporting Information Fig. S2). Considering the two pairs of *Neocrepidodera* taxa for which
307 suitability for the respective candidate hosts was included among the predictors, only from the EM
308 built from *N. cyanescens concolor* an host plant, namely *Aconitum lycoctonum*, resulted as the most
309 important predictor (Table 2). Nonetheless, the three-dimensional response surfaces represented in
310 Supporting Information Figs. S5-6 show that, at the least for one of the candidate host plants, the
311 combined effect of host suitability and of the most important bioclimatic predictor, once all the
312 remaining predictors have been set to their mean value, produced higher predicted HS values than the
313 single predictors individually did (cf. Supporting Information Figs. S3-4). Indeed, for both the *N.*
314 *cyanescens* subspecies, higher suitability values for *Aconitum lycoctonum* synergistically increase
315 suitability for the flea beetles in combination with BIO6 (*N. cyanescens concolor*) and, even though
316 less clearly, with BIO18 (*N. cyanescens cyanescens*) (Fig. S5). This pattern did not emerge
317 considering the combined effect of HS for *Aconitum napellus* and the same bioclimatic predictors.
318 With respect to the pair *N. corpulenta* – *N. rhaetica*, a positive effect on flea beetle suitability emerged
319 from the combination of *Arnica montana* suitability and BIO6 for *N. rhaetica* and, to a lesser extent,

320 from the combination of *Doronicum austriacum* suitability and mean temperature of the wettest
321 quarter (BIO8) for *N. corpulenta* (Fig. S6).

322 Continuous maps resulting from the cv EMs built for the current scenario were reported in Supporting
323 Information Fig. S7. The coefficient of variation among the predictions of the component HSMs is
324 less than 0.4 across most of the study area for *N. melanostoma*, *N. cyanescens cyanescens* and *N.*
325 *rhaetica*, while wider areas with $cv > 0.4$ emerged for *N. ligurica*, *N. cyanescens concolor* and *N.*
326 *corpulenta*, primarily outside their currently occupied range (see Figs. 2a, 3a, 4a)

327 The binarized HS under the current scenario for the three considered *Neocrepidodera* pairs and the
328 respective predicted HS shifts under the different 2070 RCP scenarios are shown in Figs. 2-4, while
329 predicted HS shifts for 2050 under the different RCPs were reported in Supporting Information Figs.
330 S8-10.

331 The core of *N. ligurica* density of occurrence in the bioclimatic space corresponds to a peripheral
332 portion of the wider density of occurrence of *N. melanostoma* (Fig. 5a2), resulting in markedly
333 broader suitable areas for this latter species also in geographical space (Figs. 2a-b). The niches of *N.*
334 *ligurica* and *N. melanostoma*, whose overlap value was $D = 0.054$, appeared not to be equivalent (P
335 < 0.001 in the niche equivalency test). However, when tested for niche divergence through the niche
336 similarity test, the niches of the two species resulted not more different than expected by chance ($P =$
337 0.652), based on differences in the bioclimatic conditions characterising the respective ranges.

338 *Neocrepidodera cyanescens concolor* and *N. cyanescens cyanescens* showed null niche overlap ($D =$
339 0) reflected by strong divergences in their occupancy of the environmental space (Fig. 5b2), which is
340 coherent with the mostly different areas predicted as suitable for them under the current scenario
341 (Figs. 3a-b). The niches of the two subspecies are clearly differentiated along the first principal
342 component, to which high contribution was given by BIO6 (Figs. 5b1-2). Moreover, the centre of the
343 occurrence density for *N. cyanescens concolor* is more shifted towards positive values of the second
344 principal component than the one for *N. cyanescens cyanescens* is, which could be due to the

345 contribution given by suitability for *Aconitum lycoctonum* to this axis (Fig. 5b1). Even though the
346 niche equivalency test rejected the hypothesis of the niches of the two *N. cyanescens* subspecies being
347 equivalent ($P < 0.001$), the niche similarity test did not permit to infer a significant divergence once
348 the differences in background conditions were considered ($P = 0.598$).

349 The niche overlap value for *N. corpulenta* and *N. rhaetica* was $D = 0.201$, reflected by their densities
350 of occurrence showing noticeable overlap but clearly separated centres (Fig. 5c2). As for the two
351 previous pairs of *Neocrepidodera*, according to the niche equivalency test the modelled niches of *N.*
352 *corpulenta* and *N. rhaetica* are not equivalent ($P < 0.001$). Anyway, the result of the niche similarity
353 test ($P = 0.562$) did not permit to reject the null hypothesis of the niches being less different than
354 expected based on the environmental conditions in the respective ranges.

355 *Neocrepidodera ligurica*, *N. cyanescens concolor*, *N. corpulenta* and *N. rhaetica* were predicted to
356 lose by 2070 the great majority of currently suitable areas, especially under RCP8.5 (Figs. 2g, 3g, 4g,
357 4h). *N. cyanescens cyanescens*, instead, was predicted to maintain under all the RCPs the major part
358 of suitable areas corresponding to the core of its current range (Figs. 3d, 3f, 3h); moreover, it was
359 predicted to gain broad suitable areas in Central and Eastern Alps under all the RCPs and in the
360 Carpathians under RCP2.6 (Fig. 3d). Finally, *N. melanostoma* was predicted to maintain stable areas
361 in Eastern Alps and potentially gain broad suitable areas even under the more pronounced warming
362 scenarios (Figs. 2d, 2f, 2h). Anyway, most of this predicted gain corresponds to areas located far
363 away from the current range of the species, while large portions of the currently occupied territories
364 were predicted to become unsuitable under RCP4.5 and RCP8.5 (Figs. 2f, 2h)

365 The variation in the extent of overlapping suitable area between each of the two *N. cyanescens*
366 subspecies and the candidate *Aconitum* hosts from the current scenario to 2050 and 2070 under the
367 three RCPs was reported, respectively, in Fig. 6a and Fig. 6c. Differently, Fig. 6b and Fig. 6d show
368 the variation in the percent extent of overlapping suitable area with respect to the overall suitable area
369 for the flea beetle under the different RCPs in 2050 and 2070. The same information for *N. corpulenta*

370 and *N. rhaetica* with respect to *Doronicum austriacum* and *Arnica montana* was summarized in Figs.
371 7a-d.

372 The overlap of suitable areas for *N. cyanescens concolor* and the two *Aconitum* species was predicted
373 to decrease both in 2050 and 2070 (Figs. 6a, 6c), with a clear negative trend along the RCP gradient
374 in 2070. The percentage of suitable area for *N. cyanescens concolor* hosting suitable conditions also
375 for *A. lycoctonum* was predicted to remain close to its current value (~ 10%) under all the three RCPs,
376 both in 2050 and 2070, while a marked decrease in the percent extent of overlapping suitable areas
377 for *N. cyanescens concolor* and *A. napellus* was predicted both in 2050 (except under RCP4.5) and
378 in 2070 (Figs. 6b, 6d).

379 Considering *N. cyanescens cyanescens*, both the extent of overlapping suitable areas with the two
380 *Aconitum* species (Figs. 6a, 6c) and the percentage of suitable area for the flea beetle hosting suitable
381 conditions also for the host plants (Fig. 6b, 6d) were predicted to decrease with respect to current
382 conditions both in 2050 and in 2070, with clearly decreasing trends along the RCP gradient emerging
383 from projections to 2070.

384 The extent of overlapping suitable areas for the pairs *N. corpulenta* – *A. montana* and *N. corpulenta*
385 – *D. austriacum* was predicted to greatly decrease with respect to current conditions under RCP4.5
386 and RCP8.5, especially in 2070 (Figs. 7a, 7c). Under RCP 8.5, in 2070 the percentage of suitable area
387 for *N. corpulenta* predicted to be suitable also for the candidate host fell to 0 both for *A. montana* and
388 for *D. austriacum* (Fig. 7d). The extent of overlapping suitable areas for *N. rhaetica* and *D.*
389 *austriacum* was almost null under the current scenario as well as in 2050 and 2070 under the different
390 RCPs (Fig. 7a, 7c). Finally, considering the pair *N. rhaetica* – *A. montana*, a decrease in both the net
391 extent and the relative percentage of overlapping suitable area with respect to the current conditions
392 emerged for all the future scenarios, except in 2050 under RCP8.5 because of the stable and gained
393 areas predicted under this scenario for *N. rhaetica* in Central and Eastern Alps (see Fig. S10), regions
394 which are suitable to *A. montana* as well (results not shown).

395

DISCUSSION

396 Given the tight bound of the considered *Neocrepidodera* taxa with the mountainous and alpine
397 ecosystems (Biondi, 1993), the identification of the variables shaping and constraining their
398 environmental niches represents an important first step to shed light on the potential future
399 distributional shifts of these flea beetles in response to the ongoing and future climate change (Bibi
400 *et al.*, 2018; Lamprecht *et al.*, 2018; Rogora *et al.*, 2018).

401 The current distributional patterns of the *Neocrepidodera* taxa within each pair are reflected in the
402 environmental niches depicted through both the Ensemble Modelling approach and the PCA-env
403 procedure.

404 *Neocrepidodera ligurica* occurs in a peripheric portion, in Western Alps, of the broader geographic
405 range of *N. melanostoma*, and the density of occurrence of the former species in the environmental
406 space indeed falls at the borders of that of *N. melanostoma* (Fig. 5a2). The narrow climatic niche of
407 *N. ligurica*, associated with its restricted current geographic range (Fig. 2a), could represent a major
408 threat to the future conservation of this species in the face of climate change (Murray *et al.*, 2010;
409 Brown & Yoder, 2015; Brunetti *et al.*, 2019). Indeed, most of the areas predicted to be suitable outside
410 the species range under the current scenario are very distant from the currently occupied ones, and
411 thus the former would be difficultly colonized; moreover, most of them are predicted to be lost even
412 under moderate warming (Figs. 2, S8). Differently, *N. melanostoma* seems to be threatened by climate
413 change only to some extent: in fact, notwithstanding the populations occurring in Western Alps may
414 suffer from the loss of suitable areas in the next decades, especially considering RCP4.5 and RCP8.5,
415 the obtained Ensemble Forecasts to 2070 predicted the gain of broad suitable areas in the northeastern
416 portion of the study area under all the considered RCPs.

417 The two *N. cyanescens* subspecies were found to occupy clearly differentiated environmental niches
418 (Figs. 5b1-2). Nonetheless, the negative result of the niche similarity test indicates that such
419 differentiation is due to the differences in the environmental conditions the two subspecies experience
420 in their respective ranges, suggesting that their divergence might have been prompted by allopatric
421 processes rather than directly by niche divergence (Pyron, 2009; McCormack *et al.*, 2010; Alvarado-
422 Serrano, 2014). *Neocrepidodera cyanescens concolor* resulted to be potentially threatened by climate
423 change as dramatically as *N. ligurica*, with major loss of currently suitable areas under RCP4.5 and
424 RCP8.5 (Figs. 3, S9). Differently, *N. cyanescens cyanescens* will likely maintain wide suitable areas
425 within the core of its current range and it is also predicted to gain some peripheral territories under
426 all the considered scenarios, which bodes well for the conservation of its current populations, at least
427 in Eastern Alps.

428 The density of occurrence in environmental space modelled for *N. corpulenta* and *N. rhaetica*
429 highlighted the existence of a certain range of environmental conditions suitable to both species, even
430 though the respective maximum density zones are clearly separated (Fig. 5c2). This is coherent with
431 the existence of a parapatric area in Western Alps where the two species currently co-occur (Iannella
432 *et al.*, 2017; Reino *et al.*, 2017). With respect to the predicted suitability shifts, both species may face
433 direct threats to the persistence of their populations in the next future: indeed, the patches of stable or
434 gained suitable areas predicted for the two species mainly under RCP 2.6 and RCP4.5, many of which
435 unlikely to be colonized due to their distance from the currently occupied areas, would difficultly
436 counterbalance the overwhelming loss of suitable territories across most of the species' range (Figs.
437 4, S10).

438 The contribution of host plant suitability resulted to be preponderant only within the Ensemble Model
439 obtained for *N. cyanescens concolor* (Table 2). Nonetheless, the three-dimensional response surfaces
440 representing the combined contribution of host suitability and influential bioclimatic variables (Figs.
441 S5-6) suggested that areas with suitable climatic conditions for the flea beetle and higher potentiality

442 of insect-plant co-occurrence may require particular attention for the conservation of some
443 *Neocrepidodera* taxa. This is particularly true considering *A. lycocotum* with respect to the two *N.*
444 *cyanescens* subspecies and *A. montana* with respect to *N. rhaetica*.

445 It is important to notice the predicted future decrease in the extent of potential co-occurrence areas
446 for almost all the considered insect-plant pairs, especially under the more pronounced warming
447 scenarios (Figs. 6-7). This could represent a double jeopardy for those flea beetles predicted to
448 experience a noticeable contraction of their potential distribution in response to warming climate, as
449 *N. cyanescens concolor*, *N. corpulenta* and *N. rhaetica*. Indeed, even though *A. montana* and *D.*
450 *austriacum* did not unequivocally emerge as important predictors of *N. corpulenta* and *N. rhaetica*
451 suitability, the reduction of potential co-occurrence under almost all the considered future scenarios
452 (Fig. 7) could represent a trend of contraction in response to warming climate common to other high-
453 altitude Asteraceae species not considered here (Dullinger *et al.*, 2012) and possibly associated to
454 these two flea beetles in a stronger manner than *D. austriacum* and *A. montana*.

455 Thus, the inclusion of variables related to biotic interactions within the HSMs confirmed to be, even
456 though not completely resolute in our study, a useful and informative praxis when applying these
457 models to conservation biogeography (Van der Putten *et al.*, 2010; Hof *et al.*, 2012; Franklin, 2013;
458 Gherghel *et al.*, 2018; Thuiller *et al.*, 2018).

459 From a conservation perspective, it should be pointed out that some of the targeted *Neocrepidodera*
460 taxa will probably require thoughtful prioritization measures in the next future. The restricted current
461 distribution of *N. ligurica* and *N. cyanescens concolor*, the narrow bioclimatic niche of the former,
462 the strong reduction of potential co-occurrence with *A. lycoctonum* predicted for the latter and the
463 dependence of both taxa on temperature-related variables (see Table 1), all represent important alarm
464 bells for the persistence of their current populations. In fact, restricted ranges and sensitivity to
465 changes in temperature regimes already emerged as strong risk factors from previous studies on other
466 orophilous endemic insects (Urbani *et al.*, 2017; Brunetti *et al.*, 2019). *N. rhaetica* and *N. corpulenta*

467 should be given appropriate consideration as well: indeed, notwithstanding they are more widely
468 distributed than the above-cited taxa, the remaining suitable areas predicted under future warming
469 conditions resulted to be far less extended and more fragmented than under current climate.

470 However, it should also be mentioned that the representation of the environmental niche emerging
471 from the implemented modelling framework may not properly represent the full fundamental niche
472 of the considered taxa. In fact, the lack of absence and/or abundance data does not permit to have a
473 complete quantification of a species niche (Brotons *et al.*, 2004; Howard *et al.*, 2014); moreover,
474 “proximal” factors other than potential host availability, like dispersal capabilities and population
475 dynamics, could have hampered the target taxa to colonize regions with suitable conditions and reach
476 the equilibrium with the environment (Guisan *et al.*, 2017).

477 In conclusion, even though detailed prioritization indications could not be provided based only on
478 HSMs forecasting (Sofaer *et al.*, 2018; Peterson *et al.*, 2018), our results highlighted the need to
479 deepen the knowledge about the threats that *Neocrepidodera* and other phytophagous insects will
480 face in the future decades. It is of the utmost importance to keep on investigating the potential effects
481 of climate change on both fauna and flora of mountainous ecosystems, encouraging the integration,
482 when possible, of modelling, experimental and field-based research.

483

ACKNOWLEDGEMENTS

We are grateful to the Editor and the two anonymous Reviewers for their insightful comments,
which permitted us to improve the clearness of this manuscript.

484 **Figures captions**

485 **Figure 1.** European biogeographical regions, as defined by the European Environmental Agency
486 (EEA), with a zoom on the study area, showing the altitudinal zonation and the occurrences for the
487 six target *Neocrepidodera* taxa and the candidate host plants.

488 **Figure 2.** Suitable areas under the current scenario, obtained from the predictions of the weighted
489 mean Ensemble Model, and α -hull-based current range (hatched polygons) for (a) *N. ligurica* and (b)
490 *N. melanostoma*; predicted shifts in habitat suitability by 2070 under RCPs 2.6, 4.5 and 8.5 for (c),
491 (e) and (g) *N. ligurica*, and (d), (f) and (h) *N. melanostoma*, respectively.

492 **Figure 3.** Suitable areas under the current scenario, obtained from the predictions of the weighted
493 mean Ensemble Model, and α -hull-based current range (hatched polygons) for (a) *N. cyanescens*
494 *concolor* and (b) *N. cyanescens cyanescens*; predicted shifts in habitat suitability by 2070 under RCPs
495 2.6, 4.5 and 8.5 for (c), (e) and (g) *N. cyanescens concolor*, and (d), (f) and (h) *N. cyanescens*
496 *cyanescens*, respectively.

497 **Figure 4.** Suitable areas under the current scenario, obtained from the predictions of the weighted
498 mean Ensemble Model, and α -hull-based current range (hatched polygons) for (a) *N. corpulenta* and
499 (b) *N. rhaetica*; predicted shifts in habitat suitability by 2070 under RCPs 2.6, 4.5 and 8.5 for (c), (e)
500 and (g) *N. corpulenta*, and (d), (f) and (h) *N. rhaetica*, respectively.

501 **Figure 5.** Contributions of the input predictors along the first two principal components ('PCA-env',
502 Broennimann *et al.*, 2012) for: (a1) *N. ligurica* and *N. melanostoma*; (b1) *N. cyanescens concolor* and
503 *N. cyanescens cyanescens*; (c1) *N. corpulenta* and *N. rhaetica*. Density of occurrence in the
504 environmental space defined by the principal components for: (a2) *N. ligurica* (Sp1) and *N.*
505 *melanostoma* (Sp2); (b2) *N. cyanescens concolor* (Sp1) and *N. cyanescens cyanescens* (Sp2); (c2) *N.*
506 *corpulenta* (Sp1) and *N. rhaetica* (Sp2). Within the density plots, solid contour lines represent the full
507 environmental background and dashed contour lines represent 50% of the background environment.

508 **Figure 6.** Variation in the extent of overlapping suitable area between the two *N. cyanescens*
509 subspecies and the corresponding candidate host plants (*Aconitum lycoctonum* and *A. napellus*) from
510 the current scenario to 2050 (a) and 2070 (c) under the three RCPs; variation in the percent extent of
511 overlapping suitable area with respect to the overall suitable area for the flea beetle under the different
512 RCPs in 2050 (b) and 2070 (d).

513 **Figure 7.** Variation in the extent of overlapping suitable area between *N. corpulenta*, *N. rhaetica* and
514 the corresponding candidate host plants (*Arnica montana* and *Doronicum austriacum*) from the
515 current scenario to 2050 (a) and 2070 (c) under the three RCPs; variation in the percent extent of
516 overlapping suitable area with respect to the overall suitable area for the flea beetle under the different
517 RCPs in 2050 (b) and 2070 (d).

518

519 **References**

- 520 Acevedo, P., Jiménez-Valverde, A., Melo-Ferreira, J., Real, R. & Alves, P. C. (2012) Parapatric species and the
521 implications for climate change studies: a case study on hares in Europe. *Global Change Biology*, **18**,
522 1509-1519.
- 523 Aiello-Lammens, M. E., Boria, R. A., Radosavljevic, A., Vilela, B. & Anderson, R. P. (2015) spThin: an R
524 package for spatial thinning of species occurrence records for use in ecological niche models.
525 *Ecography*, **38**, 541-545.
- 526 Allouche, O., Tsoar, A. & Kadmon, R. (2006) Assessing the accuracy of species distribution models:
527 prevalence, kappa and the true skill statistic (TSS). *Journal of Applied Ecology*, **43**, 1223-1232.
- 528 Alvarado-Serrano, D. F. & Knowles, L. L. (2014) Ecological niche models in phylogeographic studies:
529 applications, advances and precautions. *Molecular Ecology Resources*, **14**, 233-248.
- 530 Anderson, R. P. & Raza, A. (2010) The effect of the extent of the study region on GIS models of species
531 geographic distributions and estimates of niche evolution: preliminary tests with montane rodents
532 (genus *Nephelomys*) in Venezuela. *Journal of Biogeography*, **37**, 1378– 1393.
- 533 Araujo, M. B. & New, M. (2007) Ensemble forecasting of species distributions. *Trends Ecol Evol*, **22**, 42-47.
- 534 Archis, J. N., Akcali, C., Stuart, B. L., Kikuchi, D., & Chunco, A. J. (2018) Is the future already here? The
535 impact of climate change on the distribution of the eastern coral snake (*Micrurus fulvius*). *PeerJ*, **6**,
536 e4647.
- 537 Barbet-Massin, M., Jiguet, F., Albert, C. H., & Thuiller, W. (2012) Selecting pseudo-absences for species
538 distribution models: how, where and how many?. *Methods in ecology and evolution*, **3**, 327-338.
- 539 Baselga, A. (2006) The Northeastern Palaearctic light coloured *Neocrepidodera* Heikertinger, 1911
540 (Coleoptera: Chrysomelidae), with description of a new species. *Zootaxa*, **1246**, 55–68.
- 541 Baselga, A. & Novoa, F. (2005) The Western Palaearctic *Neocrepidodera* (Coleoptera: Chrysomelidae) of the
542 *N. impressa* and *N. ferruginea* species groups. *Annals of the Entomological Society of America*, **98**,
543 896-907.

- 544 Bibi, S., Wang, L., Li, X., Zhou, J., Chen, D., & Yao, T. (2018) Climatic and associated cryospheric, biospheric,
545 and hydrological changes on the Tibetan Plateau: a review. *International Journal of Climatology*, **38**,
546 e1-e17.
- 547 Biondi, M. (1989) Classification and phylogenesis of the Western Palaearctic species of the genus *Asiolestia*
548 Jacobson (Coleoptera, Chrysomelidae, Alticinae). *Entomography*, **6**, 519–529.
- 549 Biondi, M. (1993) Revisione del sottogenere *Asiolestia* Jacob. s. str. (Coleoptera Chrysomelidae Alticinae).
550 *Bollettino del Museo Civico di Storia Naturale di Verona*, **17**, 1–55.
- 551 Biondi, M. (2006) Chrysomelidae Alticinae. *Checklist and distribution of the Italian fauna* (ed. by Ruffo, S. &
552 Stoch, F). Memorie del Museo civico di storia naturale di Verona, 2.Serie, Sezione Scienze della Vita
553 17, with CD-ROM.
- 554 Biondi, M. & D’Alessandro, P. (2008) Taxonomical revision of the *Longitarsus capensis* species-group: an
555 example of Mediterranean-southern African disjunct distributions (Coleoptera: Chrysomelidae).
556 *European Journal of Entomology*, **115**, 719–736.
- 557 Biondi, M., Urbani, F. & D’Alessandro, P. (2015) Relationships between the geographic distribution of
558 phytophagous insects and different types of vegetation: a case study of the flea beetle genus
559 *Chaetocnema* (Coleoptera: Chrysomelidae) in the Afrotropical region. *European Journal of*
560 *Entomology*, **112**, 311–327.
- 561 Bivand, R., Keitt, T., Rowlingson, B., & Pebesma, E. (2014) rgdal: Bindings for the geospatial data abstraction
562 library. R package version 0.8-16
- 563 Brandt, L.A., Benschoter, A.M., Harvey, R., Speroterra, C., Bucklin, D., Romañach, S.S., Watling, J.I. &
564 Mazzotti, F.J. (2017) Comparison of climate envelope models developed using expert-selected
565 variables versus statistical selection. *Ecological Modelling*, **345**, 10-20.
- 566 Broennimann, O., Fitzpatrick, M. C., Pearman, P. B., Petitpierre, B., Pellissier, L., Yoccoz, N. G., Thuiller, W.,
567 Fortin, M. J., Randin, C., Zimmermann, N. E., Graham, C. H. & Guisan, A. (2012) Measuring

- 568 ecological niche overlap from occurrence and spatial environmental data. *Global Ecology and*
569 *Biogeography*, **21**, 481-497.
- 570 Brotons, L., Thuiller, W., Araújo, M. B., & Hirzel, A. H. (2004) Presence-absence versus presence-only
571 modelling methods for predicting bird habitat suitability. *Ecography*, **27**, 437-448.
- 572 Brown, J. L. & Yoder, A. D. (2015) Shifting ranges and conservation challenges for lemurs in the face of
573 climate change. *Ecology and Evolution*, **5**, 1131-1142.
- 574 Brunetti, M., Magoga, G., Iannella, M., Biondi, M., & Montagna, M. (2019) Phylogeography and species
575 distribution modelling of *Cryptocephalus barii* (Coleoptera: Chrysomelidae): is this alpine endemic
576 species close to extinction?. *ZooKeys*, **856**, 3-25.
- 577 Bucklin, D. N., Basille, M., Benscoter, A. M., Brandt, L.A., Mazzotti, F. J., Romanach, S. S., Speroterra, C. &
578 Watling, J. I. (2015) Comparing species distribution models constructed with different subsets of
579 environmental predictors. *Diversity and Distributions*, **21**, 23-35.
- 580 Burgman, M. A. & Fox, J. C. (2003) Bias in species range estimates from minimum convex polygons:
581 implications for conservation and options for improved planning. *Animal Conservation forum*, **6**, 19-
582 28
- 583 Chefaoui, R. M. & Lobo, J.M. (2008) Assessing the effects of pseudo-absences on predictive distribution
584 model performance. *Ecological Modelling*, **210**, 478-486.
- 585 Crase, B., Liedloff, A. C. & Wintle, B.A. (2012) A new method for dealing with residual spatial
586 autocorrelation in species distribution models. *Ecography*, **35**, 879-888.
- 587 D'Alessandro, P., Urbani, F. & Biondi, M. (2014) Biodiversity and biogeography in Madagascar: revision of
588 the endemic flea beetle genus *Neodera* Duvivier, 1891 with description of 19 new species
589 (Coleoptera, Chrysomelidae, Galerucinae, Alticini). *Systematic Entomology*, **39**, 710-748.
- 590 D'Alessandro, P., Samuelson, A. & Biondi, M. (2016) Taxonomic revision of the genus *Arsipoda* Erichson,
591 1842 (Coleoptera, Chrysomelidae) in New Caledonia. *European Journal of Taxonomy*, **230**, 1-61.

- 592 D'Alessandro, P., Iannella, M., Frasca, R. & Biondi, M. (2018) Distribution patterns and habitat preference
593 for the genera-group *Blepharida* s.l. in Sub-Saharan Africa (Coleoptera: Chrysomelidae:
594 Galerucinae: Alticini). *Zoologischer Anzeiger-A Journal of Comparative Zoology*, **277**, 23-32.
- 595 Di Cola, V., Broennimann, O., Petitpierre, B., Breiner, F. T., D'Amen, M., Randin, C., Engler, R., Pottier, J., Pio,
596 D., Dubuis, A., Pellissier, L., Mateo, R. G., Hordijk, W., Salamin, N. & Guisan, A. (2017) ecospat: an R
597 package to support spatial analyses and modeling of species niches and distributions. *Ecography*,
598 **40**, 774-787.
- 599 Döberl, M. (2010) Alticinae. *Catalogue of Palaearctic Coleoptera : Chrysomeloidea (Vol. 6)* (ed. by Löbl, I. &
600 Smetana, A.), pp. 491–563. Apollo Books, Stenstrup, Denmark.
- 601 Dormann, C.F. (2007) Effects of incorporating spatial autocorrelation into the analysis of species
602 distribution data. *Global Ecology and Biogeography*, **16**, 129-138.
- 603 Dormann, C. F., Elith, J., Bacher, S., Buchmann, C., Carl, G., Carré, G., Marquéz, J. R. G., Gruber, B.,
604 Lafourcade, B., Leitão, P. J., Münkemüller, T., McClean, C., Osborne, P. E., Reineking, B., Schröder,
605 B., Skidmore, A. K., Zurell, D. & Lautenbach, S. (2013) Collinearity: a review of methods to deal with
606 it and a simulation study evaluating their performance. *Ecography*, **36**, 27-46.
- 607 Dullinger, S., Gatttringer, A., Thuiller, W., Moser, D., Zimmermann, N. E., Guisan, A., Willner, W., Plutzer, C.,
608 Leitner, M. & Mang, T. (2012) Extinction debt of high-mountain plants under twenty-first-century
609 climate change. *Nature Climate Change*, **2**, 619.
- 610 ESRI 2011. ArcGIS Desktop: Release 10. Redlands, CA: Environmental Systems Research Institute.
- 611 Fielding, A. H. & Bell, J. F. (1997) A review of methods for the assessment of prediction errors in
612 conservation presence/absence models. *Environmental Conservation*, **24**, 38-49.
- 613 Forrest, J. L., Wikramanayake, E., Shrestha, R., Areendran, G., Gyeltshen, K., Maheshwari, A., Mazumdar, S.,
614 Naidoo, R., Thapa, G. J. & Thapa, K. (2012) Conservation and climate change: Assessing the
615 vulnerability of snow leopard habitat to treeline shift in the Himalaya. *Biological Conservation*, **150**,
616 129-135.

- 617 Franklin, J. (2013) Species distribution models in conservation biogeography: developments and challenges.
618 *Diversity and Distributions*, **19**, 1217-1223.
- 619 Gherghel, I., Brischoux, F. & Papeş, M. (2018) Using biotic interactions in broad-scale estimates of species'
620 distributions. *Journal of Biogeography*, **45**, 2216-2225.
- 621 Guisan, A., Lehmann, A., Ferrier, S., Austin, M., Overton, J. M. C., Aspinall, R., & Hastie, T. (2006) Making
622 better biogeographical predictions of species' distributions. *Journal of Applied Ecology*, **43**, 386-392.
- 623 Guisan, A., Thuiller, W. & Zimmermann, N. E. (2017) *Habitat Suitability and Distribution Models: With*
624 *Applications in R*. Cambridge University Press, Cambridge, UK.
- 625 Hijmans, R. J., Cameron, S. E., Parra, J. L., Jones, P. G. & Jarvis, A. (2005) Very high resolution interpolated
626 climate surfaces for global land areas. *International journal of climatology*, **25**, 1965-1978.
- 627 Hijmans, R. J. (2015) raster: Geographic Data Analysis and Modeling. R package version 2.8-19
628
- 629 Hof, A. R., Jansson, R. & Nilsson, C. (2012) How biotic interactions may alter future predictions of species
630 distributions: future threats to the persistence of the arctic fox in Fennoscandia. *Diversity and*
631 *Distributions*, **18**, 554-562.
- 632 Howard, C., Stephens, P. A., Pearce-Higgins, J. W., Gregory, R. D., & Willis, S. G. (2014) Improving species
633 distribution models: the value of data on abundance. *Methods in Ecology and Evolution*, **5**, 506-513.
- 634 Iannella, M., Cerasoli, F. & Biondi, M. (2017) Unraveling climate influences on the distribution of the
635 parapatric newts *Lissotriton vulgaris meridionalis* and *L. italicus*. *Frontiers in Zoology*, **14**, 55.
- 636 Iannella, M., Cerasoli, F., D'Alessandro, P., Console, G., & Biondi, M. (2018) Coupling GIS spatial analysis and
637 Ensemble Niche Modelling to investigate climate change-related threats to the Sicilian pond turtle
638 *Emys trinacris*, an endangered species from the Mediterranean. *PeerJ*, **6**, e4969.
- 639 Inouye, D. W. (2008) Effects of climate change on phenology, frost damage, and floral abundance of
640 montane wildflowers. *Ecology*, **89**, 353-62.
- 641 Jolivet, P. & Verma, K. K. (2002) *Biology of leaf beetles*. Intercept Ltd, Andover, U.K., 322 pp.
- 642 Kassambara, A. & Mundt, F. (2017) factoextra: extract and visualize the results of multivariate data
643 analyses. R package version 1.0.4

- 644 Konstantinov, A. S. (1991) On taxonomy of *Asiorestia* (Coleoptera, Chrysomelidae, Alticinae). [In Russian].
645 *Zoologicheskii Zhurnal*, **70**, 143–144.
- 646 Konstantinov, A. S. & Vandenberg, N. J. (1996) Handbook of Palearctic flea beetles (Coleoptera
647 Chrysomelidae Alticinae). *Contributions on Entomology, International*, **1**, 237–436.
- 648 Lamprecht, A., Semenchuk, P. R., Steinbauer, K., Winkler, M., & Pauli, H. (2018) Climate change leads to
649 accelerated transformation of high-elevation vegetation in the central Alps. *New Phytologist*, doi:
650 10.1111/nph.15290
- 651 Li, J., McCarthy, T. M., Wang, H., Weckworth, B. V., Schaller, G. B., Mishra, C., Lu, Z. & Beissinger, S.R. (2016)
652 Climate refugia of snow leopards in High Asia. *Biological Conservation*, **203**, 188-196.
- 653 Liu, C. R., White, M. & Newell, G. (2013) Selecting thresholds for the prediction of species occurrence with
654 presence-only data. *Journal of Biogeography*, **40**, 778-789.
- 655 Marmion, M., Parviainen, M., Luoto, M., Heikkinen, R. K., & Thuiller, W. (2009) Evaluation of consensus
656 methods in predictive species distribution modelling. *Diversity and distributions*, **15**, 59-69.
- 657 McCormack, J. E., Zellmer, A. J., & Knowles, L. L. (2010) Does niche divergence accompany allopatric
658 divergence in *Aphelocoma* jays as predicted under ecological speciation?: insights from tests with
659 niche models. *Evolution: International Journal of Organic Evolution*, **64**, 1231-1244.
- 660 Meinshausen, M., Smith, S. J., Calvin, K., Daniel, J. S., Kainuma, M. L.T., Lamarque, J. F., Matsumoto, K.,
661 Montzka, S. A., Raper, S. C.B., Riahi, K., Thomson, A., Velders, G. J. M. & van Vuuren, D. P. P. (2011)
662 The RCP greenhouse gas concentrations and their extensions from 1765 to 2300. *Climatic Change*,
663 **109**, 213-241.
- 664 Murray, K. A., Rosauer, D., McCallum, H., & Skerratt, L. F. (2010) Integrating species traits with extrinsic
665 threats: closing the gap between predicting and preventing species declines. *Proceedings of the*
666 *Royal Society of London B: Biological Sciences*, doi:10.1098/rspb.2010.1872.
- 667 Nadein, K. S. & Beždek, J. (2014) Galerucinae Latreille 1802. *Handbook of Zoology, Volume 4/40:*
668 *Coleoptera, Beetles, Volume 3: Morphology and Systematics (Phytophaga)* (ed. by Leschen, R.A.B. &
669 Beutel, R.G.), pp. 251–259. Walter de Gruyter Publishers, Berlin, Deutschland.

- 670 Naimi, B. (2015) usdm: Uncertainty analysis for species distribution models. R package version 1.1-12.
- 671 Pateiro-López, B. & Rodríguez-Casal, A. (2010) Generalizing the convex hull of a sample: the R package
672 alphahull. *Journal of Statistical software*, **34**, 1-28.
- 673 PESI (2018) Pan-European Species directories Infrastructure. Accessed through www.eu-nomen.eu/portal,
674 at 2018-03-31.
- 675 Peterson, A. T. & Soberon, J. (2012) Species Distribution Modeling and Ecological Niche Modeling: Getting
676 the Concepts Right. *Natureza & Conservação*, **10**, 1-6.
- 677 Peterson, A. T., Cobos, M. E., & Jiménez-García, D. (2018) Major challenges for correlational ecological
678 niche model projections to future climate conditions. *Annals of the New York Academy of Sciences*,
679 **1429**, 66-77.
- 680 Phillips, S. J., Anderson, R. P. & Schapire, R. E. (2006) Maximum entropy modeling of species geographic
681 distributions. *Ecological Modelling*, **190**, 231-259.
- 682 Pyron, R. A. & Burbrink, F. T. (2009) Lineage diversification in a widespread species: roles for niche
683 divergence and conservatism in the common kingsnake, *Lampropeltis getula*. *Molecular Ecology*,
684 **18**, 3443-3457.
- 685 R Core Team (2018) R: A language and environment for statistical computing. R Foundation for Statistical
686 Computing, Vienna, Austria. URL <https://www.R-project.org/>.
- 687 Reino, L., Ferreira, M., Martínez-Solano, Í., Segurado, P., Xu, C. & Márcia Barbosa, A. (2017) Favourable
688 areas for co-occurrence of parapatric species: niche conservatism and niche divergence in Iberian
689 tree frogs and midwife toads. *Journal of Biogeography*, **44**, 88-98.
- 690 Rogora, M., Frate, L., Carranza, M. L., Freppaz, M., Stanisci, A., Bertani, I., Bottarin, R., Brambilla, A.,
691 Canullo, R., Carbognani, M., Cerrato, C., Chelli, S., Cremonese, E., Cutini, M., Di Musciano, M.,
692 Erschbamer, B., Godone, D., Iocchi, M., Isabellon, M., Magnani, A., Mazzola, L., Morra di Cella, U.,
693 Pauli, H., Petey, M., Petriccione, B., Porro, F., Psenner, R., Rossetti, G., Scotti, A., Sommaruga, R.,
694 Tappeiner, U., Theurillat, J. P., Tomaselli, M., Viglietti, D., Viterbi, R., Vittoz, P., Winkler, M. &

- 695 Matteucci, G. (2018) Assessment of climate change effects on mountain ecosystems through a
696 cross-site analysis in the Alps and Apennines. *Science of the total environment*, **624**, 1429-1442.
- 697 Schoener, T. W. (1970) Nonsynchronous spatial overlap of lizards in patchy habitats. *Ecology*, **51**, 408-418.
- 698 Silva, D. P., Dew, R. M., Vilela, B., Stevens, M. I., & Schwarz, M. P. (2018). No deaths in the desert: predicted
699 responses of an arid-adapted bee and its two nesting trees suggest resilience in the face of
700 warming climates. *Insect Conservation and Diversity*, **11**, 449-463.
- 701 Sofaer, H. R., Jarnevich, C. S., & Flather, C. H. (2018) Misleading prioritizations from modelling range shifts
702 under climate change. *Global Ecology and Biogeography*, **27**, 658-666.
- 703 Strandberg, G., Barring, L., Hansson, U., Jansson, C., Jones, C., Kjellström, E., Kolax, M., Kupiainen, M.,
704 Nikulin, G., Samuelsson, P., Ullerstig, A. & Wang, S. (2014) *CORDEX scenarios for Europe from the*
705 *Rosby Centre regional climate model RCA4*. SMHI.
- 706 Thuiller, W., Lavorel, S., Araujo, M. B., Sykes, M. T. & Prentice, I. C. (2005) Climate change threats to plant
707 diversity in Europe. *Proceedings of the National Academy of Sciences*, **102**, 8245-8250.
- 708 Thuiller, W., Lafourcade, B., Engler, R. & Araujo, M. B. (2009) BIOMOD - a platform for ensemble forecasting
709 of species distributions. *Ecography*, **32**, 369-373.
- 710 Thuiller, W., Georges, D., Engler, R., Breiner, F., Georges, M. D. (2016) biomod2: Ensemble platform for
711 species distribution modeling. R package version 3.3–7.
- 712 Thuiller, W., Guéguen, M., Bison, M., Duparc, A., Garel, M., Loison, A., Renaud, J., Poggiato, G. & Wiersma,
713 Y. (2018) Combining point-process and landscape vegetation models to predict large herbivore
714 distributions in space and time-A case study of *Rupicapra rupicapra*. *Diversity and Distributions*, **24**,
715 352-362.
- 716 Urbani, F., D'Alessandro, P., Frasca, R., & Biondi, M. (2015) Maximum entropy modeling of geographic
717 distributions of the flea beetle species endemic in Italy (Coleoptera: Chrysomelidae: Galerucinae:
718 Alticini). *Zoologischer Anzeiger-A Journal of Comparative Zoology*, **258**, 99-109.

- 719 Urbani, F., D'Alessandro, P., & Biondi, M. (2017) Using maximum entropy modeling (MaxEnt) to predict
720 future trends in the distribution of high altitude endemic insects in response to climate change.
721 *Bulletin of Insectology*, **70**, 189-200.
- 722 Van der Putten, W. H., Macel, M., & Visser, M. E. (2010) Predicting species distribution and abundance
723 responses to climate change: why it is essential to include biotic interactions across trophic levels.
724 *Philosophical Transactions of the Royal Society of London B: Biological Sciences*, **365**, 2025-2034.
- 725 VanDerWal, J., Shoo, L. P., Graham, C. & Williams, S. E. (2009) Selecting pseudo-absence data for presence-
726 only distribution modeling: How far should you stray from what you know? *Ecological Modelling*,
727 **220**, 589-594.
- 728 Warren, D. L., Glor, R. E. & Turelli, M. (2008) Environmental niche equivalency versus conservatism:
729 quantitative approaches to niche evolution. *Evolution*, **62**, 2868-2883.
- 730 Zhang, J., Nielsen, S. E., Chen, Y., Georges, D., Qin, Y., Wang, S. S., Svenning, J.C. & Thuiller, W. (2017)
731 Extinction risk of North American seed plants elevated by climate and land-use change. *Journal of*
732 *Applied Ecology*, **54**, 303-312.

733

734

735

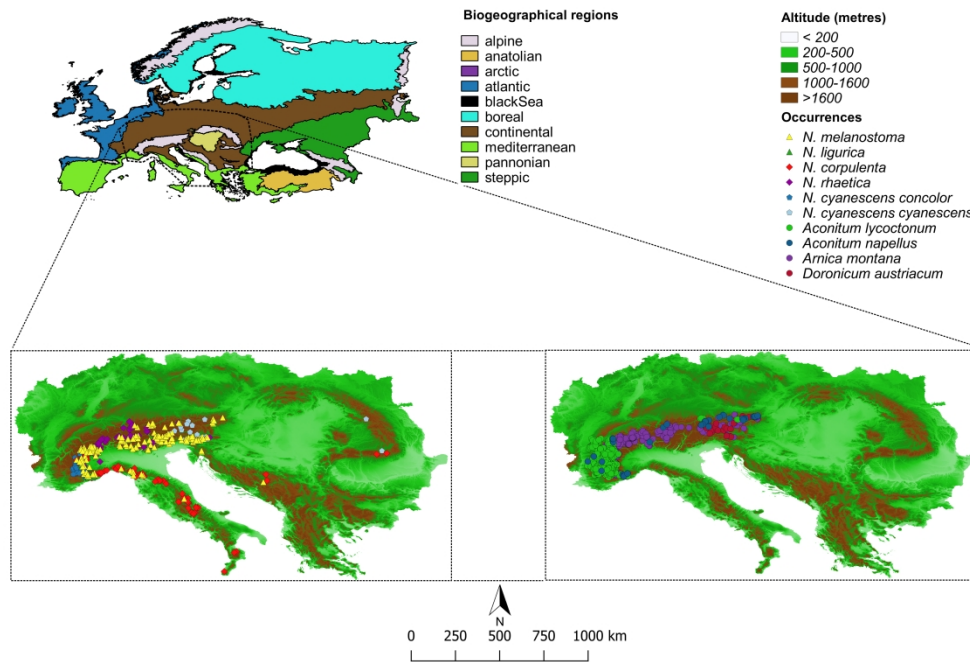


Figure 1. European biogeographical regions, as defined by the European Environmental Agency (EEA), with a zoom on the study area, showing the altitudinal zonation and the occurrences for the six target *Neocrepidodera* taxa and the candidate host plants.

222x150mm (600 x 600 DPI)

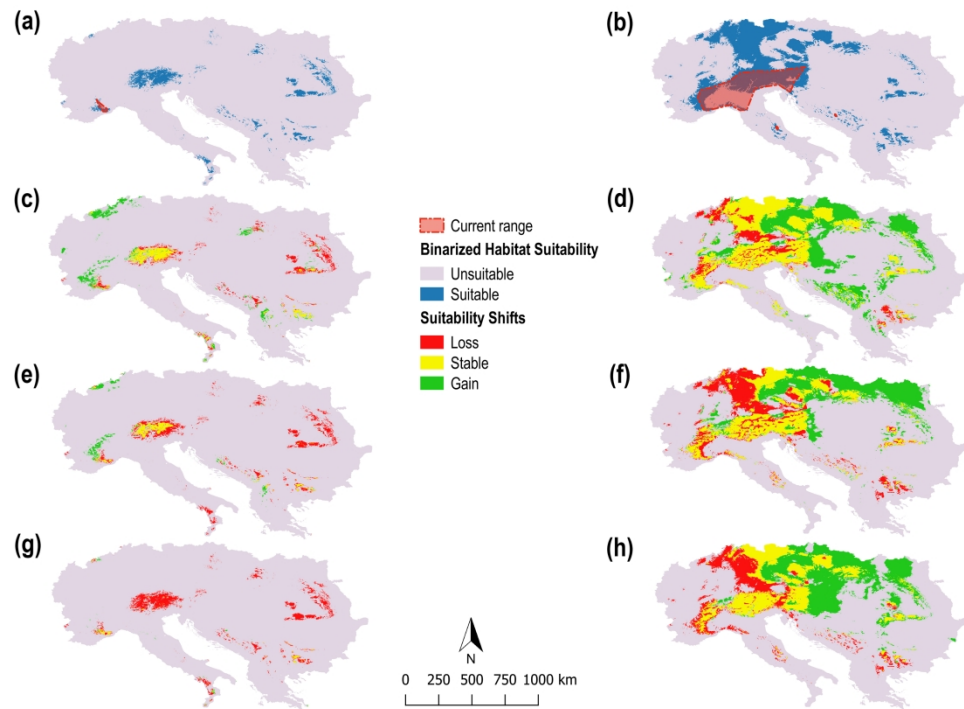


Figure 2. Suitable areas under the current scenario, obtained from the predictions of the weighted mean Ensemble Model, and α -hull-based current range (hatched polygons) for (a) *N. ligurica* and (b) *N. melanostoma*; predicted shifts in habitat suitability by 2070 under RCPs 2.6, 4.5 and 8.5 for (c), (e) and (g) *N. ligurica*, and (d), (f) and (h) *N. melanostoma*, respectively.

292x209mm (300 x 300 DPI)

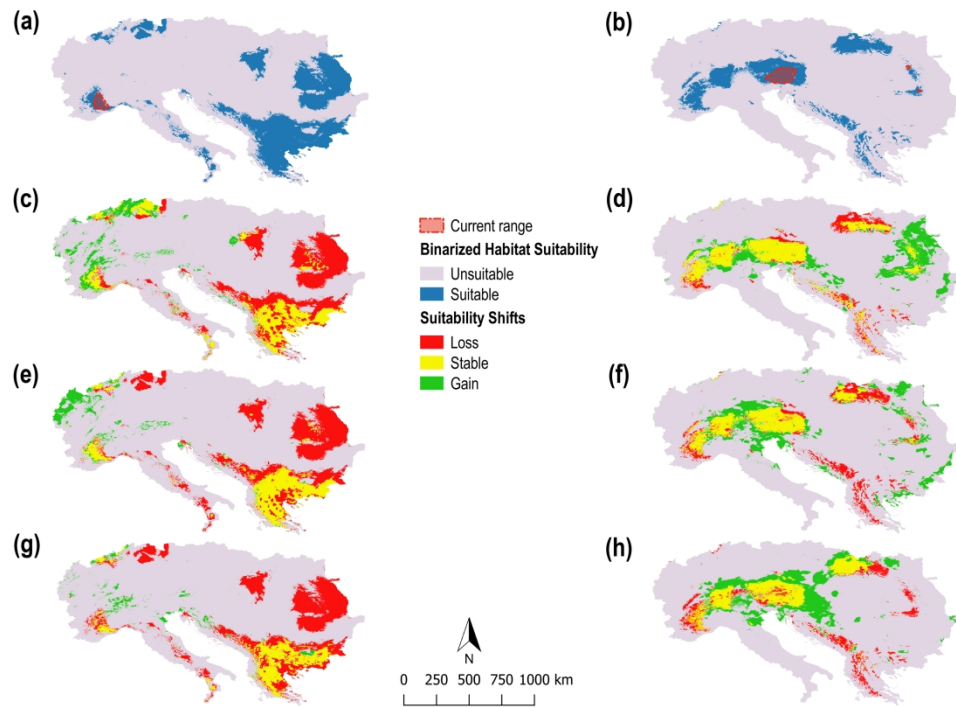


Figure 3. Suitable areas under the current scenario, obtained from the predictions of the weighted mean Ensemble Model, and α -hull-based current range (hatched polygons) for (a) *N. cyanescens concolor* and (b) *N. cyanescens cyanescens*; predicted shifts in habitat suitability by 2070 under RCPs 2.6, 4.5 and 8.5 for (c), (e) and (g) *N. cyanescens concolor*, and (d), (f) and (h) *N. cyanescens cyanescens*, respectively.

292x209mm (300 x 300 DPI)

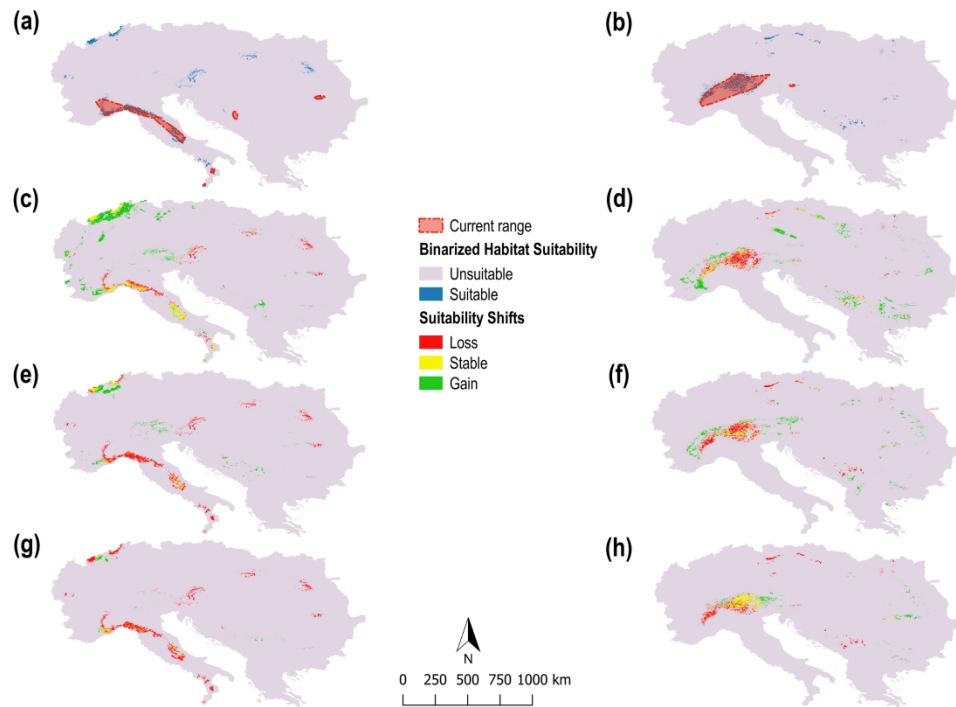


Figure 4. Suitable areas under the current scenario, obtained from the predictions of the weighted mean Ensemble Model, and α -hull-based current range (hatched polygons) for (a) *N. corpulenta* and (b) *N. rhaetica*; predicted shifts in habitat suitability by 2070 under RCPs 2.6, 4.5 and 8.5 for (c), (e) and (g) *N. corpulenta*, and (d), (f) and (h) *N. rhaetica*, respectively.

292x209mm (300 x 300 DPI)

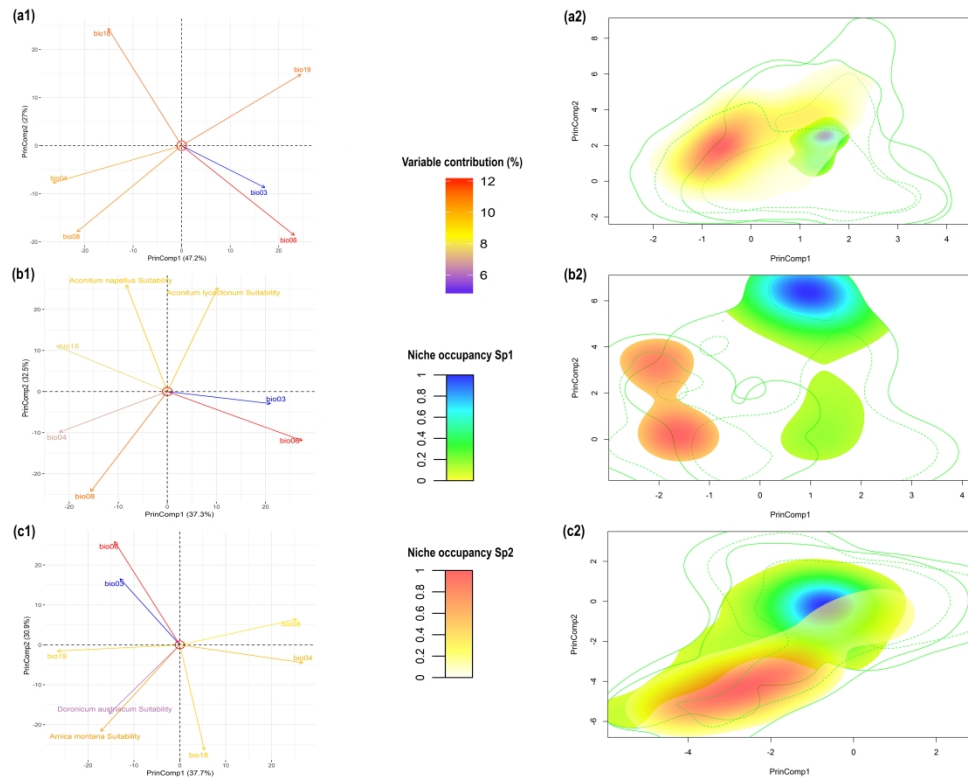


Figure 5. Contributions of the input predictors along the first two principal components ('PCA-env', Broennimann et al., 2012) for: (a1) *N. ligurica* and *N. melanostoma*; (b1) *N. cyanescens concolor* and *N. cyanescens cyanescens*; (c1) *N. corpulenta* and *N. rhaetica*. Density of occurrence in the environmental space defined by the principal components for: (a2) *N. ligurica* (Sp1) and *N. melanostoma* (Sp2); (b2) *N. cyanescens concolor* (Sp1) and *N. cyanescens cyanescens* (Sp2); (c2) *N. corpulenta* (Sp1) and *N. rhaetica* (Sp2). Within the density plots, solid contour lines represent the full environmental background and dashed contour lines represent 50% of the background environment.

228x176mm (600 x 600 DPI)

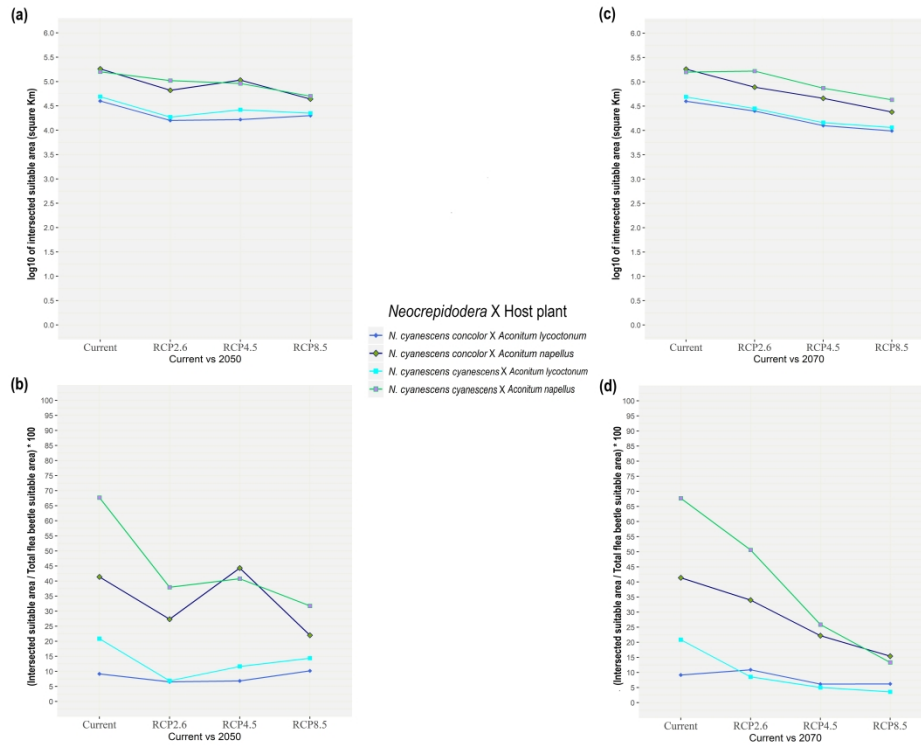


Figure 6. Variation in the extent of overlapping suitable area between the two *N. cyanescens* subspecies and the corresponding candidate host plants (*Aconitum lycoctonum* and *A. napellus*) from the current scenario to 2050 (a) and 2070 (c) under the three RCPs; variation in the percent extent of overlapping suitable area with respect to the overall suitable area for the flea beetle under the different RCPs in 2050 (b) and 2070 (d).

457x349mm (300 x 300 DPI)

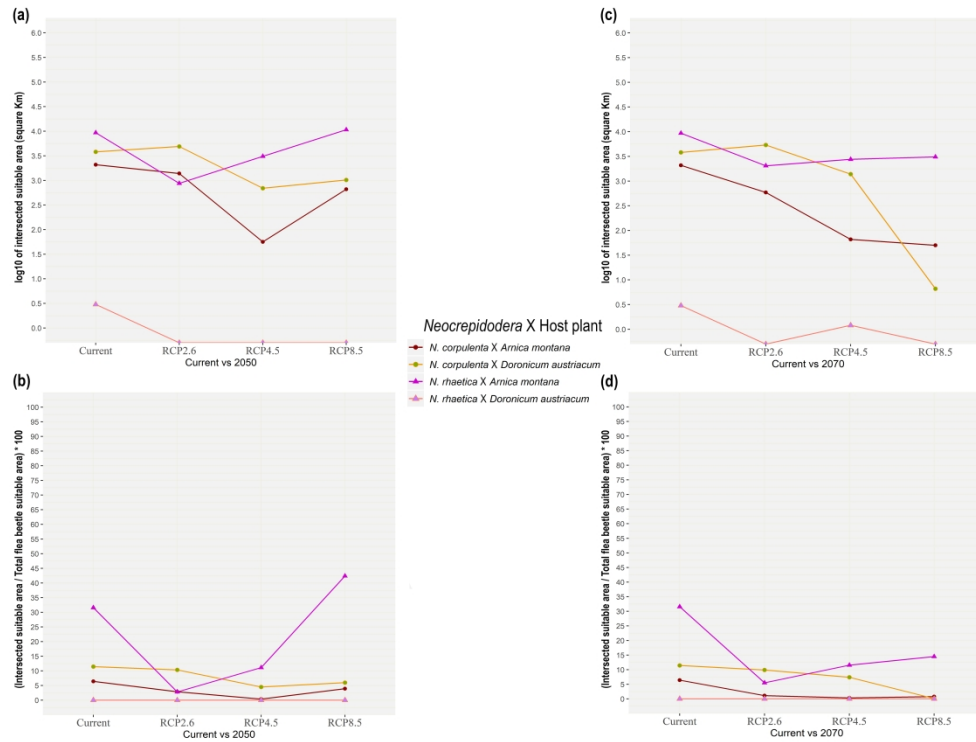


Figure 7. Variation in the extent of overlapping suitable area between *N. corpulenta*, *N. rhaetica* and the corresponding candidate host plants (*Arnica montana* and *Doronicum austriacum*) from the current scenario to 2050 (a) and 2070 (c) under the three RCPs; variation in the percent extent of overlapping suitable area with respect to the overall suitable area for the flea beetle under the different RCPs in 2050 (b) and 2070 (d).

457x349mm (300 x 300 DPI)